Rheologica Acta (2024) 63:483–491
https://doi.org/10.1007/s00397-024-01457-9

ORIGINAL CONTRIBUTION

Stress relaxation of critically fractionated entangled polybutadiene ring melts

Samruddhi Kamble[1] · Daniele Parisi[1,2,3] · Youncheol Jeong[4] · Taihyun Chang[4] · Dimitris Vlassopoulos[1,2]

Received: 31 March 2024 / Revised: 5 May 2024 / Accepted: 10 May 2024 / Published online: 28 May 2024

Abstract

We present linear viscoelastic data with anionically synthesized and critically fractionated polybutadiene (rich in vinyl content) rings having about $Z=22$ entanglements. These rings are experimentally as pure as currently possible. They exhibit a power-law stress relaxation G(t) that is well-described by the state-of-the-art fractal loopy globule (FLG) model (power-law exponent of −3/7). Previously reported data with polystyrene rings, prepared by anionic synthesis in dilute solution and purified by liquid chromatography at the critical condition, having $Z=14$ entanglements, showed a power-law G(t) as well. Recent developments with different synthetic methods yielding not so well-characterized rings with a very large number of entanglements (up to 300), suggest that a rubbery plateau emerges in the linear viscoelastic response for $Z>15$. Our work confirms the power-law G(t) with the FLG exponent with another chemistry and contributes to the current discussion about different regimes of rheological behavior, indicating that a possible deviation from the power-law FLG type of behavior toward rubbery plateau may occur for $Z>22$. To fully capture the experimental G(t) data, the FLG model is complemented by two additional relaxation modes which are attributed to ring-ring (RR) and ring-linear (RL) threading, in accordance with recent reports in the literature. The faster RR mode likely reflects a new mechanism of stress relaxation not described by FLG, and the slower RL mode is attributed to synthetic and material handling imperfections (for example, due to thermal treatment). However, it does not change the punchline of the work: no rubbery plateau for entangled rings with up to 22 entanglements.

Keywords Linear viscoelasticity · Fractal loopy globule model · Slow modes · Critical fractionation · Ring polybutadiene · Moderarely entangled polymer

Introduction

Non-concatenated ring polymers are scientifically challenging because the lack of free ends affects their conformational entropy and consequently their properties. At the same time, they serve as models that contribute not only to the understanding of biologically relevant problems such as the physics of genome folding (Grosberg 2013; Halverson et al. 2014), but also to the reinforcement of networks, triggered by loop threading and the associated constraint release mechanism (McKenna and Plazek 1986, Roovers 1988; Parisi et al. 2020).

The conventional approach to prepare macromolecular rings is to synthesize them in dilute solution (to avoid concatenation) through a ring-closure reaction from a linear α-ω functionalized precursor. Good solvent conditions reduce the probability of knot formation within a ring, likely at the expense of a larger probability to have unlinked chains at the end of the reaction (Roovers 2002; Goossen et al. 2015). To obtain reliable data, for example, viscoelastic properties, it is important to investigate rings of high purity (in particular, free from unlinked chains). It turns out that this challenge could not be satisfactorily addressed until the discovery of liquid chromatography at the critical condition (for linear chains), LCCC. This was a transformative development that led to experimentally pure rings, which were unambiguously

✉ Dimitris Vlassopoulos
dvlasso@iesl.forth.gr

[1] Institute of Electronic Structure & Laser, FORTH, 70013 Heraklion, Greece

[2] Department of Materials Science & Technology, University of Crete, 70013 Heraklion, Greece

[3] Department of Chemical Engineering, University of Groningen, Groningen 9747AG, The Netherlands

[4] Division of Advanced Materials Science and Department of Chemistry, Pohang University of Science and Technology, Pohang 37673, Korea

separated from their linear precursors (Lee et al. 2000; Chang 2005). Note however, that this synthesis and purification process yields extremely small amounts of experimentally pure rings (order of tens of milligrams) to be investigated.

Taking advantage of LCCC, it was shown that polystyrene rings (with ring closure in theta solvent) having Z = 9 and 12 entanglements exhibit a power-law stress relaxation with an exponent of −2/5, consistent with the predictions of the lattice animal model (Kapnistos et al. 2008). Note that the number of entanglements is based on the entanglement molar mass of linear chains (Ferry 1980; Fetters et al. 2007). Recently, polystyrene rings with Z = 5, 11 and 12 were prepared in good solvent and critically fractionated, and their linear viscoelastic properties were measured (Doi et al. 2015, 2017; Parisi et al. 2020, 2021). The experimental G(t) data were well-described by FLG (fractal loopy globule), the current state-of-the-art model (Ge et al. 2016):

$$G(t) = G_N^0 \left(\frac{t}{\tau_e} \right)^{-3/7} exp\left(-\frac{t}{\tau_{ring}} \right) \quad (1)$$

where G_N^0 is the rubbery plateau modulus, τ_e is the conventionally defined Rouse time of an entanglement segment, and τ_{ring} is the ring relaxation time. It should be noted that, the FLG power-law exponent of − 3/7 is very close to that of the lattice animal model (− 2/5) and not easy to discern experimentally. The exponent of − 3/7 reflects the equilibrium conformation of ring polymer melts and corresponds to a fractal exponent of 3 and stress relaxation under conditions of complete tube dilation (Ge et al. 2016). Hereafter, we only consider the FLG model. It turns out that in all situations encountered, the experimental G(t) data exhibited a slower terminal relaxation compared to the FLG prediction. The reason was the unavoidable presence of even tiny amounts of unlinked linear chains (despite the LCCC fractionation), the possible degradation of some rings due to continuous thermal treatment during measurements with small amounts of sample available (manifested as break-up of the end-link of the chains), the additional mechanism of relaxation due to ring-ring interpenetration, or a combination of these factors. In fact, even the 'ideally pure' rings obtained experimentally by multiple LCCC fractionations and extrapolation to zero contaminant concentration, were shown to exhibit a broader and slower terminal relaxation than the FLG prediction, implying that ring-ring threading is at work (Doi et al. 2017). Therefore, beyond a yet unknown molar mass threshold, the FLG mechanism cannot adequately describe the entire $G(t)$ of ring polymers, as was also recently shown experimentally and theoretically (Tu et al. 2023), and is further discussed next.

In the present work, we contribute to the challenge of unambiguously detecting experimentally the extend of molar masses exhibiting power-law relaxation of G(t). This is a problem that has been partly addressed by molecular dynamics simulations (Parisi et al. 2021; Tu et al. 2023). A natural question is whether and to what extent this power-law behavior persists when the molecular weight increases. This formidable challenge was addressed recently. Indeed, it was shown that poly(phthalaldehyde), PPA, rings can be obtained in the absence of linear contaminants since unlinking would be immediately followed by depolymerization of the chain (Tu et al. 2023). Rheological studies were performed with approximate Z values of 4, 9, 26 and 59. A clear departure from the power-law G(t) relaxation was observed for Z = 26, which became more pronounced for Z = 59. The G(t) of rings with Z = 59 was identical to that of respective linear PPA with Z = 10. The emergence of a slow mode was supported by MD simulations. In parallel, a microscopic theoretical model was proposed to explain it, by invoking the idea of inter-ring caging and drawing analogies to glassy colloidal dynamics. This approach made use of a threshold molecular weight for the emergence of caging, implying that the entanglement molecular weight may not be the only or the most appropriate metric for understanding the viscoelasticity of large ring polymers (Tu et al. 2023). Another interesting series of linear viscoelastic data was recently presented with a new chemistry, poly(3,6-dioxa-1,8-octanedithiol) rings (polyDODT), reaching an unprecedented range of Z from 23 to an ultrahigh value of 300 (Chen et al. 2023). The occurrence of a rubbery plateau was evidenced by performing careful experiments over a wide range of temperatures. By comparing the new data with respective data obtained with conventional LCCC fractionated polystyrenes, it was suggested that for Z > 15 a rubbery plateau emerges in G(t), and the respective viscosity has a much stronger molecular weight dependence compared to linear polymers (a power-law exponent of 5.8 was reported). However, some unsettled issues with the characterization of these large polymeric rings and their associated purity led the authors to call their samples 'putative cyclic polymers' (Chen et al. 2023).

From the above, it is evident that the understanding of the stress relaxation of experimentally pure rings up on increasing molecular weight and the possible deviations from the self-similar response is an outstanding challenge. This work contributes by presenting linear viscoelastic data with LCCC-purified polybutadienes having Z = 22. We find that there is no rubbery plateau and the FLG mechanism is still at work, while two additional slow modes are necessary to describe the entire stress relaxation.

Materials and methods

Synthesis and characterization

Polybutadiene (PB) with predominantly 1,2-content (vinyl) was synthesized by anionic polymerzation. A α,ω telechelic linear chain was synthesized in dilute solution (to avoid concatenation) in good solvent tetrahydrofuran (THF)

using potassium naphthalenide as initiator, at −78℃. These conditions typically yield a vinyl content of about 70% (Bywater et al. 1984). The α,ω telechelic PB anions were end-capped with diphenyl ethylene and subsequent radical coupling using potassium naphthalenide yielded cyclization products. The synthetic scheme is presented in Figure 1 below and details are presented in the Appendix. The cyclization product contains multiple rings and various linear adducts in addition to single rings (Ziebarth et al. 2016), as seen in the gel permeation chromatography (GPC) data of Figure 6 of the Appendix. It was fractionated by a two-step liquid chromatography (LC) separation process. First, LC at critical condition (LCCC) was performed at 21.4℃ (two 250 × 10 mm Nucleosil C18 columns, 100 Å/5 µm and 300 Å/7 µm; CH_2Cl_2/CH_3CN (78/22, v/v) at a flow rate of 2 mL/min) to fractionate the linear precursor and its adducts from the rings (Figure 2A). The LCCC fractionation successfully fractionated the ring products from linear polymers, but the ring product still contained various multiple rings (Figure 7 of the Appendix). Next, an interaction chromatography (IC) separation was performed at 15℃ (one 250 × 10 mm Nucleosil C18 column, 100 Å/5 µm and CH_2Cl_2/CH_3CN (78/22, v/v) at a flow rate of 1.8 mL/min) to fractionate single rings from multiple rings (Figure 2B).

The final product (Figure 8 of the Appendix) had a weight-average molar mass $M_w = 85{,}000$ g/mol, as measured by GPC-light scattering detection, and a polydispersity of 1.02. Based on the measured plateau modulus of the linear precursor (see Figure 3A and discussion below) and rubber elasticity theory, the entanglement molar mass was estimated to be $M_e = 3890$ g/mol, yielding $Z = 22$ entanglements. These numbers suggest a higher vinyl content (exceeding 90%; see Fetters et al. 2007) than originally anticipated based on synthesis, mentioned above. Unfortunately, we did not measure the vinyl content by ^{1}H-NMR and the small specimen degraded after multiple heating cycles so it could not be used further, but this limitation does not affect the punchline of the work. Hereafter, we denote the ring PB by R85 and its linear precursor by L85.

Rheometry

We used an ARES strain-controlled rheometer (TA, USA) with stainless steel plate-plate geometry (diameters of 4 and 8 mm, typical gap of about 0.45 mm), and temperature controlled (±0.1℃) via a convection oven fed with gas and liquid nitrogen, to achieve a range from −10 to 65℃. The samples were thermally equilibrated at each measurement temperature (as confirmed by dynamic time sweep tests) and the frequency-dependent moduli were recorded by imposing oscillatory strains of small amplitude (typically 1%) to ensure linear response (checked with dynamic strain sweep tests). The frequency range was 100–0.01 rad/s. The data at different temperatures were superimposed to create a master curve. Note also that the high-frequency (low-temperature) data in the glassy region were corrected to account for compliance effects as discussed in the literature (Laukkanen 2017). Based on calibration, a compliance factor of J = 0.02 rad/Nm was used (Alexandris et al. 2020).

Results and discussion

Figure 3A shows the linear viscoelastic (LVE) master curves of the measured linear and ring polybutadienes at a reference temperature $T_{ref} = 25$℃. Master curves were obtained via time–temperature superposition, indicating the (expected) thermorheological simplicity of these polymers. The horizontal and vertical shift factors are depicted in Fig. 3B and are invariant to the macromolecular architecture. The temperature-dependent horizontal shift factors were fitted

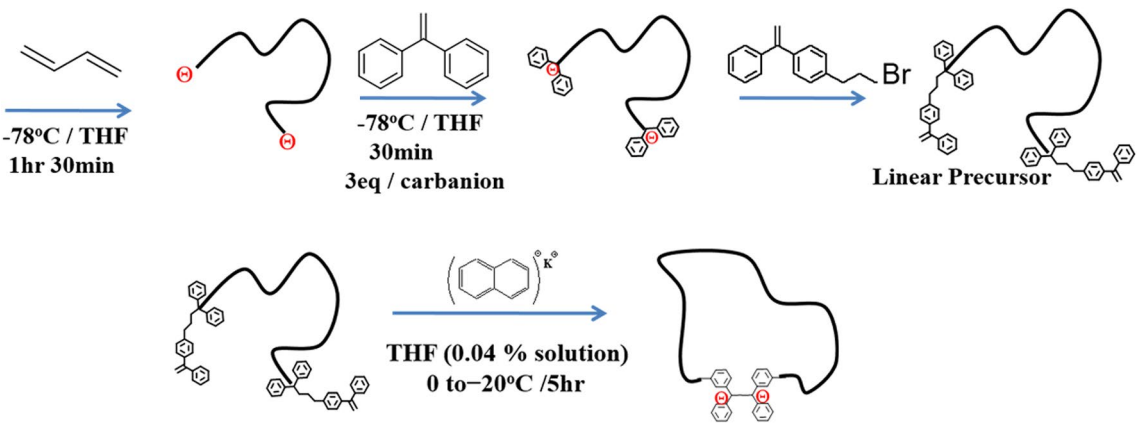

Fig. 1 Schematic describing the synthesis of a telechelic linear polybutadiene precursor (top) and its end-coupling to obtain the ring (bottom)

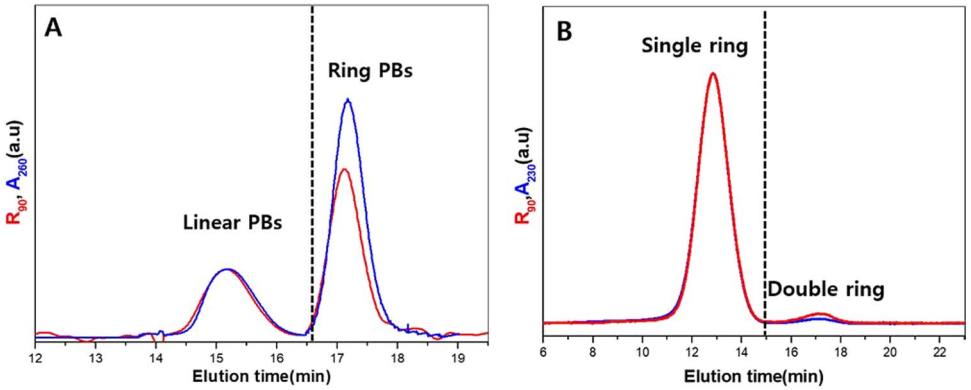

Fig. 2 Typical PB chromatograms obtained from the two-step liquid chromatography approach: **A** LCCC signals separating rings from linear chains. **B** IC signals separating the single ring from the multiple rings, yielding the purified single rings. R_{90} is the Rayleigh ratio (normalized LS intensity) at the scattering angle of 90° and A_{260} (A_{230}) is the absorbance at the wavelength of 260 (230) nm. PB does not absorb at 260 nm. The A_{260} signal comes from the phenyl groups (from DPE) at the chain ends

with the William-Landel-Ferry (WLF) equation, yielding $C_1 = 6.6$ and $C_2 = 70$ K. For the temperature dependence of the density, we used the relation taken from Mark (2007): $\rho(T) = 0.876e^{-6.75 \cdot 10^{-4} \cdot T(^\circ C)}$ (g/cm^3). The prime observation from Fig. 3A is that, unlike its linear precursor, the ring does not exhibit a rubbery plateau, but instead relaxes in a power-law fashion as discussed in the literature (Kapnistos et al. 2008) and explained below. Indeed, in the frequency range between about 10^3 rad/s and about 10^{-1} rad/s, the ring exhibits a decay of both the storage (*G'*) and loss (*G"*) moduli, which are nearly identical. Actually, careful observation of the data indicates that *G'* slightly exceeds *G"* (hence, the onset of the terminal regime is marked by a moduli crossover). This can be attributed to the presence of small amounts or remaining impurities (discussed below), but it could be also possible that at $Z = 22$, we may approach the threshold for the transition to another relaxation regime that is characterized by the eventual emergence of rubbery plateau that cannot be excluded, but cannot be fully confirmed either. The unambiguous finding is the absence of rubbery plateau in R85, as clearly evidenced by the comparison of its LVE master curve with that of L85 in Fig. 3A. Some additional remarks are in order. The fact that the high-frequency data of the ring and the linear precursor collapse is a confirmation of the good quality of the data since, for this molar mass the two architectures have the same glass transition temperature (Yang and Di Marzio 1991; Pasquino et al. 2013; Pipertzis et al. 2022). Furthermore, the terminal regimes of R85 and L85 are very different. In the latter case, one can clearly observe a well-defined relaxation process due to reptative and non-reptative moves. On the other hand, the former case is characterized by a very broad relaxation process, that is typical of entangled rings and will be elucidated below.

To better appreciate the data and assess the quality of the obtained master curves, we show in Figure 4 the more

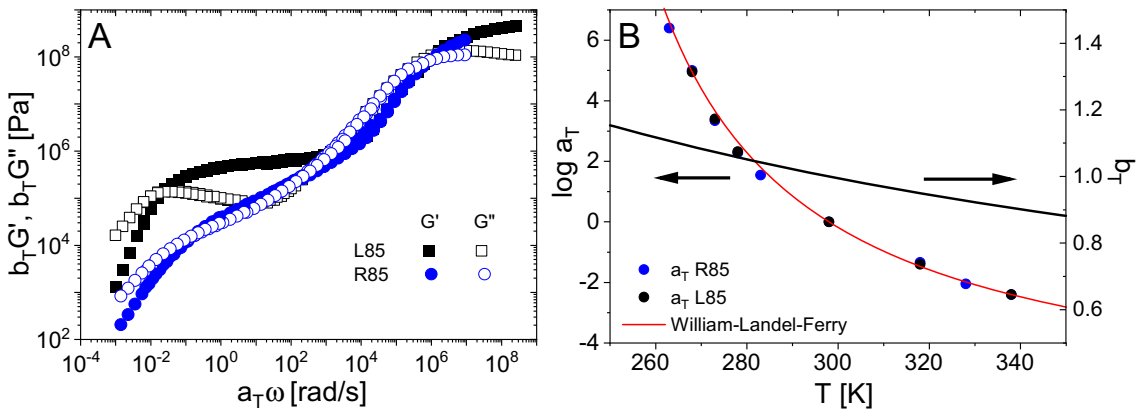

Fig. 3 **A** LVE master curves of the PB ring R85 and its linear precursor L85, at a reference temperature $T_{ref} = 25$℃. **B** Temperature dependent horizontal (a_T) and vertical (b_T) shift factors used to construct the master curve of **A**. The line through the $a_T(T)$ data is the WLF equation (see text for details)

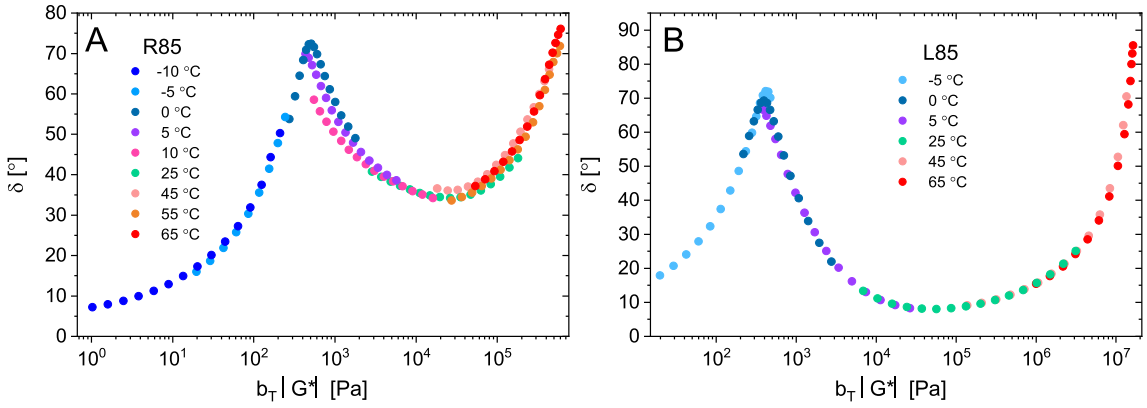

Fig. 4 Van Gurp-Palmen representation of the LVE data of Fig. 3 for (**A**) PB ring R85 and (**B**) its linear precursor L85, at various temperatures (see legend)

sensitive van Gurp–Palmen representation. The collapse of the R85 data is very good, albeit not perfect; in particular that data at 10℃ clearly deviate from the rest. This can be attributed to experimental issues (for example sample equilibration at this temperature or slight error in adjusting the plates and gap to account for thermal expansion). However, this does not affect the message, i.e., the ring is thermorheologically simple and it does not exhibit a rubbery plateau.

The data of Fig. 3A are replotted in the form of $G(t)$ in Fig. 5. The conversion from dynamic modulus $G^*(\omega)$ to stress relaxation modulus $G(t)$ was performed via the Schwarzl's method (Schwarzl 1975; Parisi et al. 2020). Here, we focus only at times $t > \tau_e$, well beyond the segmental relaxation. In this range, the respective data of the linear precursor exhibit a transient rubbery plateau and eventual terminal relaxation. This is well described by the state-of-the-art Likhtman-McLeish (LM) (2002) model, as indicated in the figure. The LM model was implemented in the Mathematica® software by using the experimental values of τ_e and G_N^0, equally to 0.5 ms (at 25 °C) and 0.57 MPa, respectively, $M_e = 3890$ g/mol, and the constraint release parameter $c_v = 0.1$. The respective ring data are first fitted with the FLG model (Eq. (1)). The power-law relaxation is well-described and the data comply with the power-law exponent of − 3/7, extending for over 4 decades in time, more that the model. On the other hand, the model visibly underpredicts the terminal relaxation (Fig. 5). This overall behavior is consistent with that observed with polystyrene rings with smaller Z (Parisi et al. 2021; Doi et al. 2017). The origin of this deviation can be attributed to different reasons, as explained above, and further experimental analysis is a true challenge. We seem to have reached the limits of current experimental capabilities. As seen in Fig. 5,

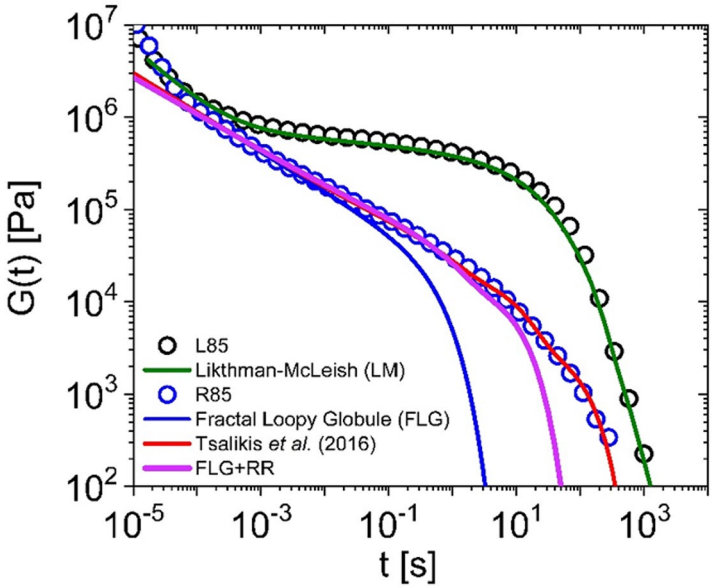

Fig. 5 Experimental $G(t)$ data at times $t > \tau_e$ for the linear precursor L85 and the ring R85 polybutadiene ($T_{ref} = 25$℃). The lines are respective fits with models as indicated in the legend: for linear polymers Likhtman-McLeish (LM), and for the rings: Fractal Loopy Globule (FLG), FLG with one slow contribution due to ring/ring (RR) interpenetration, FLG with two slow modes, RR and ring/linear (RL) (Tsalikis et al. 2016). For details see text

the experimental G(t) is fitted satisfactorily with the addition of slow modes as per Eq. (2) below (Tsalikis et al. 2016):

$$G(t) = G_N^0\left(\frac{t}{\tau_e}\right)^{-3/7} exp\left(-\frac{t}{\tau_{ring}}\right) + +G_{N,RR}\sum_{p:odd}\frac{8}{p^2\pi^2}exp\left(-\frac{p^2t}{\tau_{RR}}\right) + G_{N,RL}\sum_{p:odd}\frac{8}{p^2\pi^2}exp\left(-\frac{p^2t}{\tau_{RL}}\right) \quad (2)$$

where the second and third right-hand terms of this equation are the relaxation modes with respective intensity and relaxation times associated with threading mechanisms between rings (G_{RR},τ_{RR}) and ring and linear chains (G_{RL},τ_{RL}). Table 1 below reports the experimental and fitting parameters used with Eq. (2). The ring relaxation time τ_{ring} has been assigned to the inverse frequency at the dynamic moduli crossover (Fig. 3A). The plateau modulus of the linear precursor has been identified as the storage modulus value at the minimum of the loss factor, reaching a value of 0.57 MPa, in agreement with reported values for high vinyl content polybutadiene (Fetters et al. 2007). Since the RR mechanism seems to be inherent to pure rings and to affect their dynamics more as their molar mass increases (Tsalikis et al. 2016; Tu et al. 2023), while the RL mechanism likely reflects imperfections (incomplete purification and/or ring unlinking in the present case), we also show in Fig. 5 the fit of the data with the FLG model and one relaxation mode, representing the RR contribution (keeping the same values for G_{RR} and τ_{RR}, see Table 1). It is evident that the agreement with the data is clearly improved with respect to the single FLG fit, indicating that the FLG model does not capture the complete physics of ring relaxation at high molar masses.

Note that whereas the assignment of the faster RR and slower RL modes seems to be somehow arbitrary, it is triggered by detailed simulations of threading events (Tsalikis and Mavrantzas 2014, 2020; Tsalikis et al. 2016), which suggest that RL threadings are more persistent (long-living) compared to RR threadings. This is also consistent with the current understanding of the ring-linear constraint release mechanism that delays the dynamics of the blend substantially (Parisi et al. 2020). We emphasize that at this stage, this is a reasonable hypothesis and that the real value is, this analysis is the good fit of the experimental G(t) with the incorporation of two relaxation mechanisms in addition to the FLG mode.

The ratio $G_{\text{RR}}/G_{\text{RL}}$ (about 4) can be thought of as a rough estimate of the relative strength of the two slow modes or else, even with fewer RL threading events, their relaxation is slower, because they are deeper (Parisi et al. 2020). The extracted zero-shear viscosity of R85 from the fitted experimental data (entire G(t) curve) as discussed above is 678.7 kPa.s and FLG mode contribution is 37.9 kPa.s. For comparison, the zero-shear viscosity of L85 is 16.2 MPas. It is therefore clear that the emergence of slow modes and their contribution to the viscoelastic relaxation of ring polymers remains an open problem. So is the purity of rings, which at the moment can be properly addressed only by simulations. However, the latter are currently limited vis a vis the size of polymers to be investigated. Nevertheless, the clear message from the present investigation is the up to $Z = 22$, experimentally pure rings do not exhibit a rubbery plateau. The power-law G(t) is validated for different chemistries.

Conclusions

We have investigated the linear viscoelastic response of specially synthesized, experimentally pure (critically fractionated) polybutadiene (1,2-addition) rings having about $Z = 22$ entanglements. Unlike their linear precursors, these rings do not exhibit a rubbery plateau. Their viscoelastic stress relaxation function G(t) exhibits a power-law decay, that is well-described by the state-of-the-art fractal loopy globule (FLG) model with a power-law exponent of −3/7. However, to fully describe the entire G(t), two slow modes were added, attributed to the ring-ring and ring-linear threading events, consistent with simulations and recent experimental developments. The faster of the two modes is attributed to ring-ring interpenetration and likely reflects an additional mechanism not described by FLG. On the other hand, the slower mode is attributed to ring-linear interpenetration and reflects experimental imperfections (ring unlinking and remaining linear contaminants not removed during the fractionation process). This study extends the range of ring molar masses that exhibit power-law stress relaxation by 50%, using experimentally pure rings. The previous limit was $Z = 14$ and achieved with polystyrene. Hence, the use of polybutadiene with low entanglement molar mass is promising, though the purification process, possible remaining traces of unlinked chains, and possible degradation due to unlinking of rings subjected to continuous thermal and mechanical treatments are constant experimental concerns. In addition, our results suggest that a possible threshold for deviation from the power-law FLG type of behavior toward a rubber plateau regime should occur for $Z > 22$. Obtaining well-characterized experimental rings with larger Z and deeper analysis by simulations are the current formidable challenges in the field.

Table 1 Model parameters extracted from fitting the G(t) ring data of Fig. 5 with Eq. (2)

Experiments			Fitting parameters			
τ_{ring} (s)	G_N^0(MPa)	τ_e (s)	τ_{RR} (s)	τ_{RL} (s)	G_{RR} (Pa)	G_{RL} (Pa)
1.2	0.57	0.0005	10	100	18,500	4500

Appendix

I. Synthesis of polybutadiene

The polymerization procedure is essentially the same as in Ziebarth et al. (2016) except for the monomer. The initiator, potassium naphthalenide, was synthesized by the reaction between potassium (Aldrich, 99%) and naphthalene (Aldrich, 99%) in tetrahydrofuran (THF) at room temperature for 5 h. 1,1-Diphenylethylene (DPE, Hokko Chemicals, 95%) was dried over calcium hydride first and treated with n-BuLi before vacuum distillation. 1-(4-(3-Bromopropyl)phenyl)-1-phenylethylene (DPE-Br) was synthesized according to the method of Higashihara et al. (2005). All polymerizations and reactions were carried out in an Ar atmosphere. The preparation scheme of telechelic polybutadiene (PB) with a DPE functional group at both ends is shown in Scheme 1 of the manuscript. Anionic polymerization of butadiene was initiated by potassium naphthalenide in THF at −78 °C. After 1.5 h of polymerization, THF solution of DPE (0.5 mol/L) was added for end-capping at a molar ratio of [DPE]/[K^+] ~ 3 and was allowed to react for 30 min. Then THF solution of DPE-Br (0.5 mol/L) was added at a molar ratio of [DPE-Br]/[K^+] ~ 3 at −78 °C. The end-capped linear PB precursors were precipitated in an excess amount of methanol and then reprecipitated in acetonitrile to remove the residual DPE and DPE-Br. The ring closure by radical coupling reaction of the PB precursors was carried out by slowly introducing potassium naphthalenide (0.07 mol/L) in THF into a very dilute THF solution (0.4 g/L) of the PB precursor at a molar ratio of [DPE]/[K^+] ~ 1/5 and stirred for 5 h. After quenching with dried methanol, the polymer was precipitated in an excess amount of methanol.

Note that the double bond in the vinyl group in the PB backbone is far less reactive than the double bond of DPE. Therefore, the anion radicals formed at DPE by the reaction with potassium naphthalenide react with each other by radical coupling exclusively. We may not exclude the possibility of the reaction backbone vinyl group completely, but the following LC separation and the characterization results (both main and side products) show that the reaction of the vinyl group in the backbone can be ignored. In addition, the initiation reaction of the PB polymerization utilizes the same chemistry of the reaction of butadiene with potassium naphthalenide, in which formed anion radicals of butadiene molecules undergo radical coupling to form dianions of dibutadiene to grow bidirectionally without side reaction.

II. Characterization of the polybutadiene rings (chromatograms)

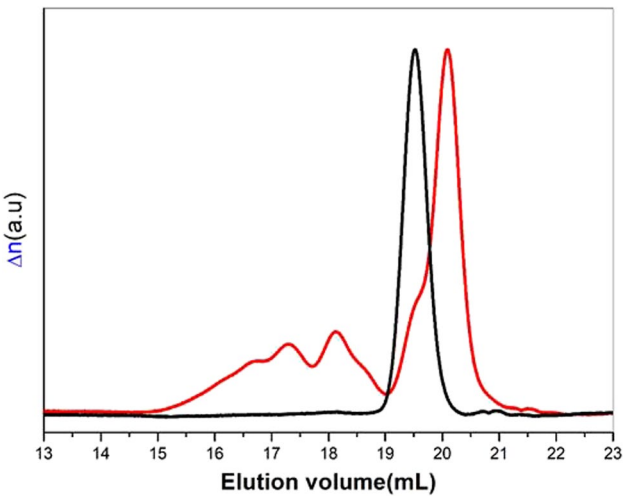

Fig. 6 GPC chromatograms of the cyclization product (red) vs. linear precursor (black). The major peak of the cyclization product shifts to the longer retention volume (19.5 mL to 20.1 mL), reflecting the smaller hydrodynamic volume of the ring relative to the linear precursor. In addition, the cyclization product contains various byproducts including unreacted precursors, high molar mass linear adducts and multiple rings. (Columns: Polypore + Jordi Gel DVB Mixed + Waters DVB, Flow rate: 0.7 mL/min)

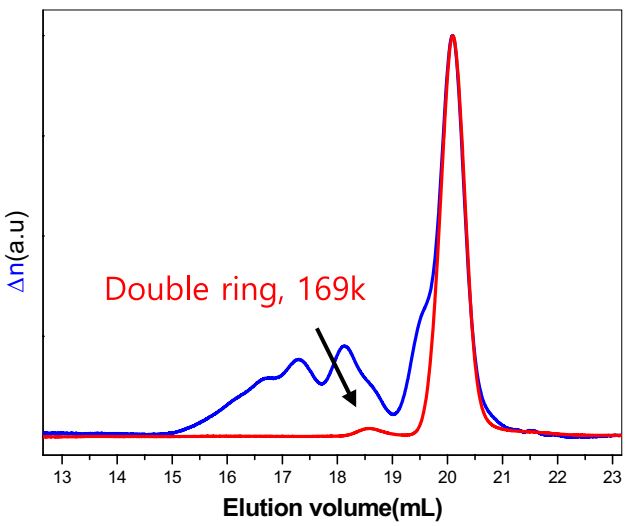

Fig. 7 GPC chromatogram of the cyclization product before (blue) and after (red) the LCCC fractionation. The LCCC fractionation (Fig. 2A) can separate the linear PBs from the ring PB, but the fractionated ring PB still contains multiple rings. (Columns: Polypore + Jordi Gel DVB Mixed + Waters DVB, Flow rate: 0.7 mL/min)

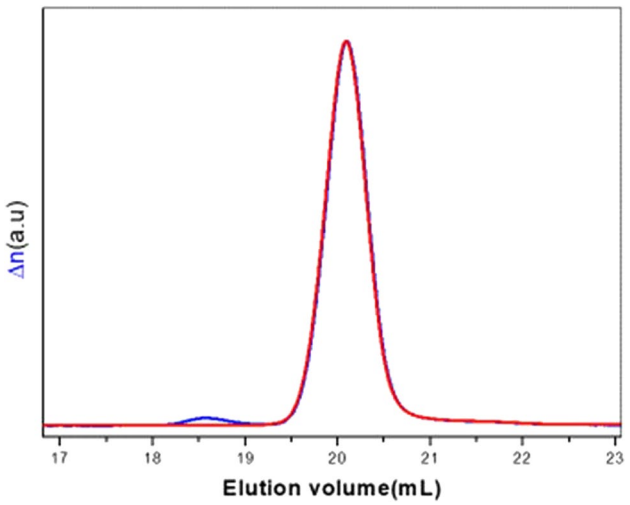

Fig. 8 GPC chromatogram of the ring PB before (blue) and after (red) the IC fractionation. The IC fractionation (Fig. 2B) can separate the single ring PBs from the multiple ring PB yielding the pure single ring PB. (Columns: Polypore + Jordi Gel DVB Mixed + Waters DVB, Flow rate: 0.7 mL/min)

Acknowledgements This research was supported by the Hellenic Foundation for Research and Innovation (H.F.R.I.) under the "Second Call for H.F.R.I. Research Projects to support Faculty members and Researchers" (project number: 4632).

Data Availability Data presented in this work can be available upon reasonable request.

References

Alexandris S, Peponaki K, Petropoulou P, Sakellariou G, Vlassopoulos D (2020) Linear viscoelastic response of unentangled polystyrene bottlebrushes. Macromolecules 2020(53):3923–3932

Bywater S, Firat Y, Black PE (1984) Microstructure of PBs prepared by AP in polar solvents. Ion-pair and solvent effects. J Polym Sci Polym Chem Ed. 22(3), 669–672

Chang T (2005) Polymer characterization by interaction chromatography, J Polym Sci: Part B Polym Phys. 43, 1591–1607

Chen D, Molnar K, Kim H, Helfer CA, Kaszas G, Puskas JE, Kornfield JA, McKenna GB (2023) Linear viscoelastic properties of putative cyclic polymers synthesized by reversible radical recombination polymerization (R3P). Macromolecules 56:1013–1032

Doi Y, Matsubara K, Ohta Y, Nakano T, Kawaguchi D, Takahashi Y, Takano A, Matsuhita Y (2015) Melt rheology of ring polystyrenes with ultrahigh purity. Macromolecules 48:3140–3147

Doi Y, Matsumoto A, Inoue T, Iwamoto T, Takano A, Matsushita Y, Takahashi A, Watanabe H (2017) Re-examination of terminal relaxation behavior of high-molecular-weight ring polystyrene melts. Rheol Acta 56:567–581

Ferry JD (1980) Viscoelastic properties of polymers, 3rd Ed., Wiley

Fetters LJ, Lohse DJ, Colby RH (2007) Chain dimensions and entanglement spacing, in Mark, J. E. Physical Properties of Polymers, 2nd Ed., Springer

Ge T, Panyukov S, Rubinstein M (2016) Self-similar conformations and dynamics in entangled melts and solutions of nonconcatenated ring polymers. Macromolecules 49:708–722

Goossen S, Brás AR, Pyckhout-Hintzen W, Wischnewski A, Richter D, Rubinstein M, Roovers J, Lutz PJ, Jeong Y, Chang T, Vlassopoulos D (2015) Influence of the solvent quality on ring polymer dimensions. Macromolecules 48:1598–1605

Grosberg AY (2013) Annealed lattice animal model and Flory theory for the melt of non-concatenated rings: towards the physics of crumpling. Soft Matter 10:560–565

Halverson JD, Smrek J, Kremer K, Grosberg AY (2014) From a melt of rings to chromosome territories: the role of topological constraints in genome folding. Rep Prog Phys 77:022601

Higashihara T, Nagura M, Inoue K, Haraguchi N, Hirao A (2005) Successive synthesis of well-defined star-branched polymers by a new iterative approach involving coupling and transformation reactions. Macromolecules 38(11):4577–4587

Kapnistos M, Lang M, Vlassopoulos D, Pyckhout-Hintzen W, Richter D, Cho D, Chang T, Rubinstein M (2008) Unexpected power-law stress relaxation of entangled ring polymers. Nat Mater 7:997–1002

Laukkanen O-V (2017) Small-diameter parallel plate geometry: a simple technique for measuring rheological properties of glassforming liquids in shear. Rheol Acta 56:661–671

Lee HC, Lee LH, W., Chang, T., Roovers, J. (2000) Fractionation of cyclic polystyrene from linear precursor by HPLC at the chromatographic critical condition. Macromolecules 33:8119–8121

Likhtman AE, McLeish TCB (2002) Quantitative theory for linear dynamics of linear entangled polymers. Macromolecules. 35, 6332.6343

Mark JE (ed) (2007) Physical properties of polymers handbook, 2nd edn. Springer, New York

McKenna GB, Plazek DJ (1986) The viscosity of blends of linear and cyclic molecules of similar molecular mass. Polymer Commun 27:304–306

Parisi D, Ahn J, Chang T, Vlassopoulos D, Rubinstein M (2020) Stress relaxation in symmetric ring-linear polymer blends at low ring fractions. Macromolecules 53:1685–1693

Parisi D, Costanzo S, Jeong Y, Ahn J, Chang T, Vlassopoulos D, Halverson JD, Kremer K, Ge T, Rubinstein M, Grest GS, Srinin W, Grosberg AY (2021) Nonlinear shear rheology of entangled polymer rings. Macromolecules 54:2811–2827

Pasquino R, Vasilakopoulos TC, Jeong YC, Lee H, Rogers S, Sakellariou G, Allgaier J, Takano A, Brás AJ, Chang T, Gooβen S, Pyckhout-Hintzen W, Wischnewski A, Hadjichristidis N, Richter D, Rubinstein M, Vlassopoulos D (2013) Viscosity of ring polymer melts. ACS Macro Lett 2:874–878

Pipertzis A, Ntetsikas K, Hadjichristidis N, Floudas G (2022) Cyclic topolohies in linear –dihydroxy polyisoprenes by dielectric spectroscopy. Macromolecules 55:10491–10501

Roovers J (1988) Viscoelastic properties of polybutadiene rings. Macromolecules 21:1517–1521

Roovers J (2002) Organic cyclic polymers, in Cyclic Polymers, 2nd Ed., ed. J. A. Semlyen, (Kluwer Academic Publishers, Dordrecht, The Netherlands)

Schwarzl FR (1975) Numerical calculation of stress relaxation modulus from dynamic data for linear viscoelastic materials. Rheol Acta 14(7):581–590

Tsalikis DG, Mavrantzas VG (2014) Threading of ring poly(ethylene oxide) molecules by linear chains in the melt. ACS Macro Lett 3:763–766

Tsalikis DG, Mavrantzas VG, Vlassopoulos D (2016) Analysis of slow modes in ring polymers: threading of rings controls long-time relaxation. ACS Macro Lett 5:755–760

Tsalikis DG, Mavrantzas VG (2020) Size and diffusivity of polymer rings in linear polymer matrices: the key role of threading events. Macromolecules 53:803–820

Tu MQ, Davydovich O, Mei B, Singh PK, Grest GS, Schweizer KS, O'Connor TC, Schroeder CM (2023) Unexpected slow relaxation dynamics in pure ring polymers arise from intermolecular interactions. ACS Polym Au 3(4):307–317

Yang AJ-M, Di Marzio EA (1991) Glass temperature of polymer ring systems. Macromolecules 24:6012–6018

Ziebarth JD, Gardiner AA, Wang Y, Jeong Y, Ahn J, Jin Y, Chang T (2016) Comparison of critical adsorption points of ring polymers with linear polymers. Macromolecules 49:8780–8788